Geophysical Research Letters

RESEARCH LETTER
10.1029/2023GL104163

Robust Relationship Between Midlatitudes CAPE and Moist Static Energy Surplus in Present and Future Simulations

Ziwei Wang[1,2] **and Elisabeth J. Moyer**[1,2]

[1]Department of the Geophysical Sciences, University of Chicago, Chicago, IL, USA, [2]Center for Robust Decision-making on Climate and Energy Policy (RDCEP), University of Chicago, Chicago, IL, USA

Key Points:

- Convective available potential energy (CAPE) shows a strong dependence on "moist static energy surplus" and this dependence holds across climate states. These results are robust across models
- Shifts in CAPE contours under climate change mean that hotter and/or wetter conditions are required to produce a given CAPE
- Distributional shifts in future midlatitudes CAPE can be well-captured given 3 regional mean changes: surface T and RH, and upper-level T

Supporting Information:

Supporting Information may be found in the online version of this article.

Correspondence to:

E. J. Moyer,
moyer@uchicago.edu

Citation:

Wang, Z., & Moyer, E. J. (2023). Robust relationship between midlatitudes CAPE and moist static energy surplus in present and future simulations. *Geophysical Research Letters*, *50*, e2023GL104163. https://doi.org/10.1029/2023GL104163

Received 17 APR 2023
Accepted 20 MAY 2023

Abstract Convective available potential energy (CAPE), a metric associated with severe weather, is expected to increase with warming, but we have lacked a framework that describes its changes in the populated midlatitudes. In the tropics, theory suggests mean CAPE should rise following the Clausius–Clapeyron (C–C) relationship at ∼6%/K. In the heterogeneous midlatitudes, where the mean change is less relevant, we show that CAPE changes are larger and can be well-described by a simple framework based on moist static energy surplus, which is robust across climate states. This effect is highly general and holds across both high-resolution nudged regional simulations and free-running global climate models. The simplicity of this framework means that complex distributional changes in future CAPE can be well-captured by a simple scaling of present-day data using only three parameters.

Plain Language Summary Severe thunderstorms cause substantial damage and may become more destructive in the future. Because these events are associated with conditions of high "Convective Available Potential Energy" (CAPE), it is important to understand how CAPE might increase in a future warmer climate. However, existing theories designed for the tropics are not suitable for the U.S. and similar areas. We find that future changes in CAPE are complex and cannot be predicted based on surface temperature alone, but can be explained using three factors: temperature and moisture at the surface and temperature at a higher level. A single simple framework is therefore able to explain CAPE differences between present and future climates, warm and cold regions, and daytime and nighttime.

1. Introduction

Convective Available Potential Energy (CAPE), loosely defined as the vertically integrated buoyancy of a near-surface air parcel, is a metric closely associated with extreme convective weather events that can cause substantial socioeconomic damages (e.g., Johns et al., 1992). CAPE is derived from the difference between the temperature profile of a parcel rising pseudo-adiabatically from the surface and that of the background environment (Moncrieff & Miller, 1976), which determines the maximum possible updraft velocity during undiluted ascent. In meteorology, CAPE is used to predict thunderstorm events and in particular hail (Groenemeijer & van Delden, 2007; Kaltenböck et al., 2009; Kunz, 2007). Studies have also used the covariate of CAPE and wind shear to explain differences in thunderstorm frequency across locations (Brooks et al., 2003, 2007) or across climate states (Diffenbaugh et al., 2013; Trapp et al., 2009).

Early efforts to understand CAPE in observations sought to characterize it as a function of near-surface temperature and moisture (Williams & Renno, 1993; Ye et al., 1998). More recent studies of CAPE in observations have tended to focus on decadal-scale trends, often finding large increases. For example, Gettelman et al. (2002) found trends equivalent to ∼50%/K in 15 tropical radiosonde stations. Model studies of CAPE under climate change have tended to produce smaller effects. Several recent studies that simulate the tropics using convection-permitting models (0.2–4 km resolution) without advection, that is, approximating radiative-convective equilibrium (RCE), find CAPE increases of 8%/K (Muller et al., 2011), 8%/K (Romps, 2011), 12%/K (Singh & O'Gorman, 2013), 7%/K (Seeley & Romps, 2015), and 6%–7%/K from theory (Romps, 2016). In the midlatitudes, changes may be larger. K. L. Rasmussen et al. (2017) show 11%/K for three stations in the Eastern U.S.; Diffenbaugh et al. (2013) and Chen et al. (2020) show ∼10%/K over the Eastern U.S.; and Lepore et al. (2021) find 10%–14%/K for the entire U.S. These results are consistent across a wide range of model resolutions.

Theoretical frameworks to explain climatological CAPE fall into two groups. One approach assumes that background environmental profiles are fully determined by surface temperature, and predicts them by considering the

effects of convective entrainment. Singh and O'Gorman (2013) proposed a "zero-buoyancy model" based on the assumption that entrainment makes actual buoyancy in an ascending convective plume small relative to CAPE (with column RH considered fixed). Singh and O'Gorman (2015) and Zhou and Xie (2019) extended the work and validated the approach under RCE. However, the theory is not expected to work for midlatitudes land, which has strong spatial and temporal variations, even though its climatological mean profile is close to RCE (Miyawaki et al., 2022).

A second approach treats surface and mid-tropospheric conditions as independent variables. Emanuel and Bister (1996) (henceforth EB96) drew on heat engine theory and described the relationship as

$$CAPE = A \cdot (h_s - h_m) \tag{1}$$

where h_s and h_m are moist static energy (MSE) near the surface (boundary layer) and in the mid-troposphere, respectively. In this perspective, CAPE represents the maximum possible kinetic energy that can be released given a heat transfer of $(h_s - h_m)$, and CAPE is generated only when surface MSE exceeds that of a mid-tropospheric threshold. Agard and Emanuel (2017), Li and Chavas (2021) (hereafter, AE17 and LC21) modified the approach to use a different threshold term, dry static energy, and showed that results captured aspects of CAPE variations in the midlatitudes.

We modify the framework based on Emanuel (1994) and use as the threshold term the minimum "saturation MSE" h_m^* in the mid-troposphere, the moist static energy a parcel would have if saturated:

$$CAPE = A \cdot (h_s - h_m^*) \tag{2}$$

We term the difference $h_s - h_m^*$ the "MSE surplus." The integral form of this expression can be derived from the definition of CAPE given the assumption that the effect of water vapor on buoyancy is negligible. (See Text S1 and Figure S1 in Supporting Information S1.) We then simplify to a linear dependence (as in e.g., AE17) by replacing the integral with a difference at a single location. This assumption is valid as long as the shape of the environmental temperature profile does not vary strongly with h_s and can be folded into the slope A. The rationale for h_m^* as the threshold term can also be expressed intuitively: CAPE depends only on temperature differences, and above the level of free convection, the rising parcel is saturated and conserves h^*, so its difference with the environment should be taken with a comparable quantity. Zhang and Boos (2023) used h_m^* as a threshold for convective instability over summertime mid-latitude land, but Equation 2 has not yet been evaluated as a framework for CAPE.

A sufficiently general framework should explain not only average CAPE, or CAPE in the average profile, but its variations across space and time in the highly heterogeneous midlatitudes. This generality is required for any application to extreme weather, since only the high tail of CAPE is associated with the severe thunderstorms that produce large socioeconomic impacts. Although no prior work has addressed future changes in midlatitudes CAPE distributions, studies suggest they may shift in complex ways. For example, Chen et al. (2020) show that spatial patterns of CAPE changes over North America differ from those of present-day CAPE.

In this work, we use observations and model simulations to evaluate how CAPE changes under CO_2-induced warming, and to test whether the relationship of Equation 2 captures these changes. That is, we ask whether it robustly applies to current and future CAPE distributions across climate states. Furthermore, we ask whether robustness means that complex distributional changes can be reproduced by as few as three parameters derived from regional means. Our goal is to quantify changes in CAPE distributions in the midlatitudes and to provide a simple framework that explains them.

2. Data and Methods

2.1. Model Output

Most analysis here uses high-resolution model output: a paired set of present and future dynamically downscaled simulations over continental North America from the Weather Research and Forecasting model (WRF, version 3.4.1) run at 4 km resolution. Both runs are described in Liu et al. (2017) and are acquired from NCAR RDA (Rasmussen & Liu, 2017). The present-day simulation (CTRL) uses ERA-Interim reanalysis for initial and boundary conditions and for a large-scale spectral nudging (scales >2,000 km) applied to levels above the planetary boundary layer, to match planetary-scale weather patterns. Small-scale processes can still evolve freely. The

future simulation is a pseudo-global-warming (PGW) scenario, treated identically but with reanalysis adjusted by a spatially—and temporally—varying offset derived from the CMIP5 multi-model mean projection under RCP8.5, to reflect large-scale changes under increased CO_2. These runs have been validated against observations (Wang et al., 2021) and used in studies of future CAPE changes (Sun et al., 2016; K. L. Rasmussen et al., 2017). In this work, we use the years 2001–2012 and the equivalent future period.

To test whether results apply generally to a diverse set of free-running models, we use 11 CMIP6 models, selected based on the availability of the 6-hourly output needed for CAPE calculation. Models have widely varying mean CAPE, from 704 to over 2461 J/kg in summertime N America, with the best performance (MPI-ESM1-2-LR) comparable to WRF at ∼30 versus 14 J/kg bias against IGRA (Chavas & Li, 2022; Wang et al., 2021). We use pairs of historical (2005–2014) and ssp585 (2091–2100) simulations (Eyring et al., 2016). To allow comparison with observations, we subset all model output to 80 grid points that match International Global Radiosonde Archive (IGRA) weather stations in North America, as in Wang et al. (2021). For consistency, we calculate surface-based CAPE in all runs using the same python package. For "paired" comparisons, we match each profile in CTRL/historical with its equivalent in PGW/ssp585. As in prior studies, most analyses here use only the summertime (MJJA or JJA), when convection is most active.

2.2. Methods: Regressions and Subsetting

All linear fits in this work are made using binned median data, to homogenize CAPE sampling. All fits are computed using orthogonal distance regression (ODR), which is most appropriate in conditions where errors in both dependent and independent variables matter. See Schwarzwald et al. (2021) for discussion of ODR. When fitting to estimate the fractional change in CAPE between climate states, we use the entire data set, and we divide by the overall mean temperature change (4.65 K in WRF runs) when giving values in %/K. However, many comparisons focus on convective conditions and therefore involve a subset of the data. For regressions of CAPE against MSE surplus, we impose an absolute cut at CAPE >1,000 J/kg. In other cases we compute values for profiles above the 73rd quantile in CAPE, which corresponds to CAPE >1000 J/kg in the WRF CTRL run. When constructing synthetic profiles, we apply a temperature offset derived from profiles with CAPE >73rd percentile in each climate state (3.92 K in WRF runs), to best capture the change in convective conditions.

2.3. Synthetic Profiles

To help understand the minimal information needed to reproduce future CAPE changes, we construct three synthetic CAPE distributions based on the WRF CTRL profiles.

1. For *Clausius-Clapeyron* scaling, shown for illustrative purposes only, we simply multiply each CTRL CAPE value by 1.33 ($=e^{0.061 \cdot 4.65}$, where 6.1%/K is C–C for the mean temperature of high-CAPE profiles, 301.8 K). We neglect several factors whose systematic effects on CAPE would largely cancel: the projected rise in the Level of Neutral Buoyancy (LNB) (+0.6%/K); the reduction in surface RH (−0.4%/K), and treating profiles separately (−0.1%/K).
2. For the *constant offset* case, we add a fixed temperature offset of 3.92 K to each CTRL profile at each level from surface to 200 hPa (near the LNB in the mean CTRL profile), then linearly interpolate to zero change at 75 hPa. We show cases with and without a surface RH adjustment of −0.9%, the mean change for profiles with CAPE >73rd quantile.
3. For the *lapse rate adjustment* case, we modify the *constant offset* procedure to also include a change in lapse rate $\Gamma = (T_s - T_{200})/z_{200}$. That is, we linearly interpolate between a warming of 3.92 K at the surface and a similarly-derived 4.94 K at 200 hPa. We also apply the −0.9% surface RH adjustment.

For context, we also show predictions of the SO13 theory under a 4.65 K temperature rise. We derive entrainment rate parameters of 0.67 and 0.68 for the WRF CTRL and PGW runs, and use true LNB values for each profile. (Singh and O'Gorman (2013) used a fixed entrainment parameter of 0.75 and a fixed LNB temperature of 200 K.)

3. Results

3.1. Changes in CAPE Distributions

We begin our analysis by asking: in midlatitudes model projections, how much and how does CAPE change with warming? In the WRF model runs, average summertime CAPE rises by 10% per degree of warming (a 61% increase, from 684 to 1,103 J/kg with a mean surface temperature rise of 4.65 K). However, an alternate approach that emphasizes changes in higher-CAPE conditions may be more appropriate, and we use it throughout this work.

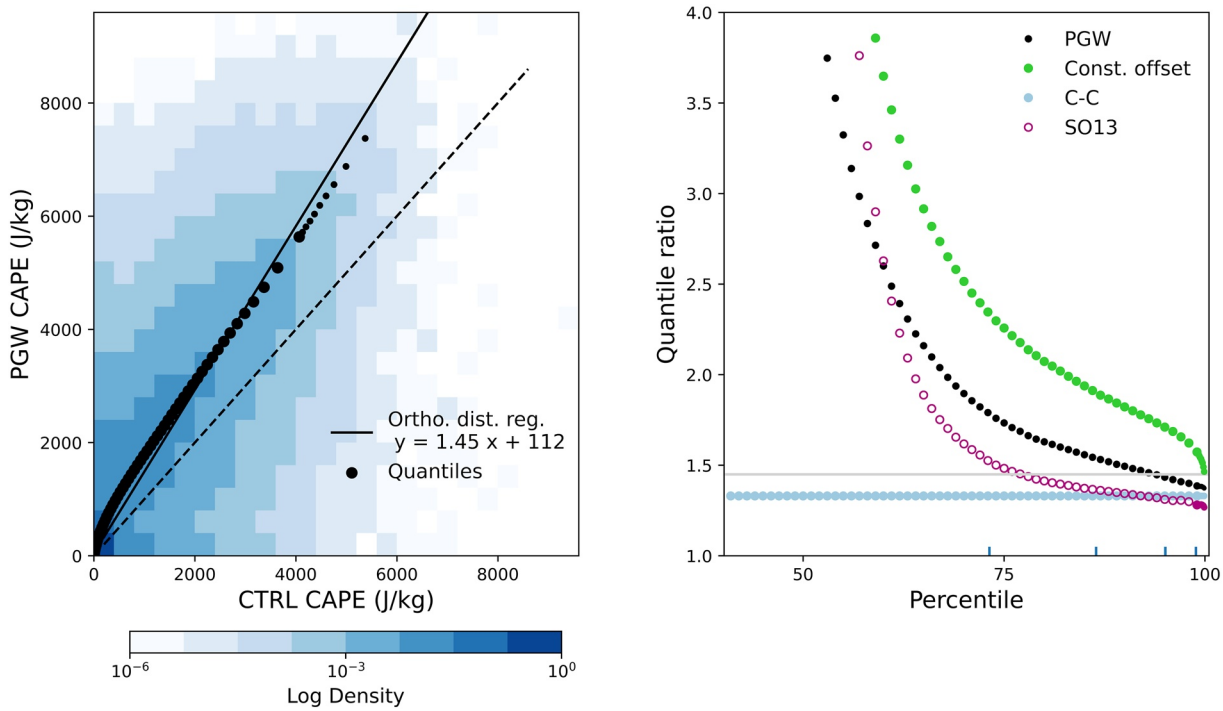

Figure 1. (Left) Comparison of CAPE in present (CTRL) and future (PGW) model runs as a density plot of paired profiles (see Methods), showing also the 1:1 line (dashed); the orthogonal regression (solid); and quantiles of the distribution (large dots, 1% increments from 0 to 0.99; small dots 0.1% increments above 0.99). (Right) Quantile ratio plot, constructed by taking the ratio of future to present CAPE quantiles, showing WRF output (black, same dots as L. panel), the synthetic datasets *C-C scaling* (light blue) and *constant offset* (light green), and for reference *SO13* (purple, with changes computed relative to its own CTRL distribution). Gray horizontal line marks the +45% mean change from the orthogonal regression. Four vertical tick bars mark the percentiles matching 1,000, 2,000, 3,000, and 4,000 J/kg (73.2%, 86.5%, 95.1%, and 98.9%, respectively). The x-axis is truncated to omit quantiles where CTRL CAPE is zero. Changes in WRF are smaller than those in *constant offset*, implying some lapse rate adjustment.

We perform an orthogonal regression on the density distributions of paired profiles in present and future runs, which yields a clear shift upwards even though weather systems are not identical in the two runs and the scatter is therefore large (Figure 1, left). The slope yields a CAPE increase of 8.0%/K (45% total). With either method, the change is larger than in Clausius Clapeyron (6.1%/K) or in the SO13 theory developed for the tropics (6.0%/K), but smaller than would result from simply changing surface values while leaving atmospheric profiles unchanged (11.7%/K in the *constant offset* synthetic, which adds a single ΔT to all levels in all profiles; see Figure S2 in Supporting Information S1). Midlatitudes atmospheric lapse rates have therefore lessened slightly in the future simulation, as expected.

Distributional effects in future CAPE changes can be readily seen by comparing values for individual quantiles to the overall regression line (Figure 1, left, dots). The lower quantiles lie above the regression line and the extreme high-CAPE quantiles (>~3,000 J/kg) below it, meaning the future CAPE distribution is narrower than that produced by a simple mean shift. This relative narrowing manifests as a downward slope in a quantile regression plot, which shows the ratio of individual quantiles of future versus present-day CAPE (Figure 1, right). The effect is a necessary result of the nonlinear CAPE—temperature relationship: a given temperature rise produces a greater effect in low-CAPE conditions. For this reason, relative narrowing occurs even when surface temperature increases are uniform and environmental profiles do not change (*constant offset*, green) or in a theoretical approach that does not use observed environmental profiles (SO13, purple).

3.2. The Effect of Changes in Environmental Profiles

We found in Section 3.1 that environmental adjustments appear to reduce future CAPE increases. To isolate this effect, we examine mean CAPE in surface temperature and humidity (T–H) space, following Wang et al. (2021) (Figure 2). Since surface T and H uniquely define the moist adiabat on which a parcel rises, a change in CAPE for a given T–H is due only to an altered environmental profile. This approach effectively decomposes CAPE changes into a sampling effect and a partially compensating lapse rate effect. In the WRF model runs used here,

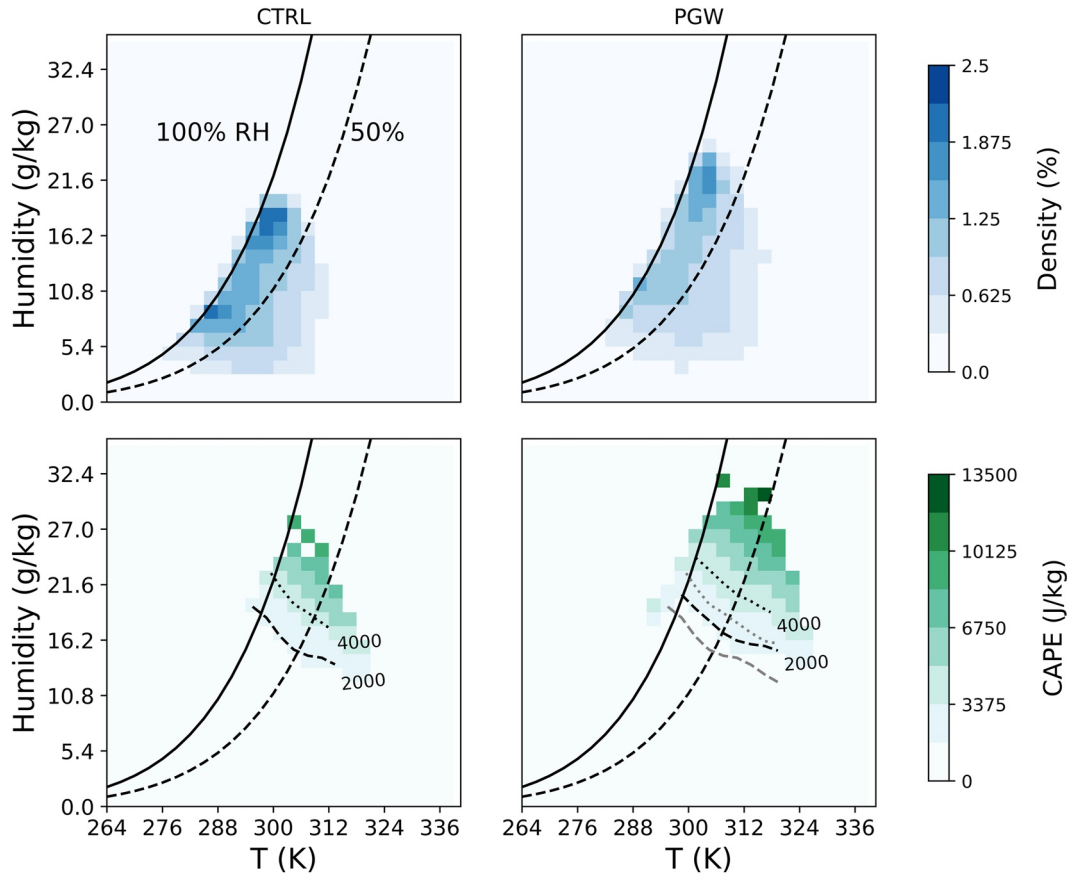

Figure 2. Density heatmaps of (top) sampling of T–H bins and (bottom) mean CAPE in each T–H bin, in CTRL (left) and PGW (right) WRF runs during summer (MJJA). Bins shown are all those with three or more observations. Solid and dashed lines mark RH of 100% and 50%. In the bottom row, dashed/dotted lines mark CAPE contours at 2,000 and 4,000 J/kg, with CTRL contours repeated in PGW panel as gray lines. Although conditions sampled in PGW are hotter than in CTRL (top), each given T,H bin is associated with smaller CAPE (bottom).

increased sampling of hot and humid surface conditions in PGW would more than double CAPE from its CTRL values if environmental profiles remained constant (Figure 2, top), but environmental changes nearly halve that increase (Figure 2, bottom). This environmental damping makes future CAPE smaller for each T–H bin, so that hotter or wetter surface conditions are needed to achieve the same CAPE.

Most of this damping results from subtle changes in environmental profiles. Lapse rates across the domain lessen by 3% between CTRL and PGW, from −6.56 to −6.35 K/km (for the CAPE >73rd quantile subset). However, some damping also occurs even if the lapse rate distribution remains fixed (Figure S3 in Supporting Information S1). Because lapse rates in our domain are correlated with temperature—binned averages range from −5 K/km at 270 K to over −7 K/km at 320 K—then as the surface warms, each given temperature become associated with more stable conditions (Figure S4 in Supporting Information S1). The combined result is that CAPE contours in T–H space shift substantially between CTRL and PGW.

We can immediately make two inferences about CAPE changes in our model runs. First, because CAPE contours align with those of MSE (Figure S5 in Supporting Information S1), CAPE in our data set must be strongly related to surface MSE. Second, because CAPE contours in T–H space shift while MSE by definition cannot, this relationship must shift in future simulations. Both effects are consistent with Equation 2.

3.3. CAPE-MSE Surplus Framework

As predicted, the relationship between CAPE and surface MSE is reasonably linear in each climate state and shifts as the climate warms (Figure 3, top left). That is, CAPE on average does not develop unless surface MSE (h_s)

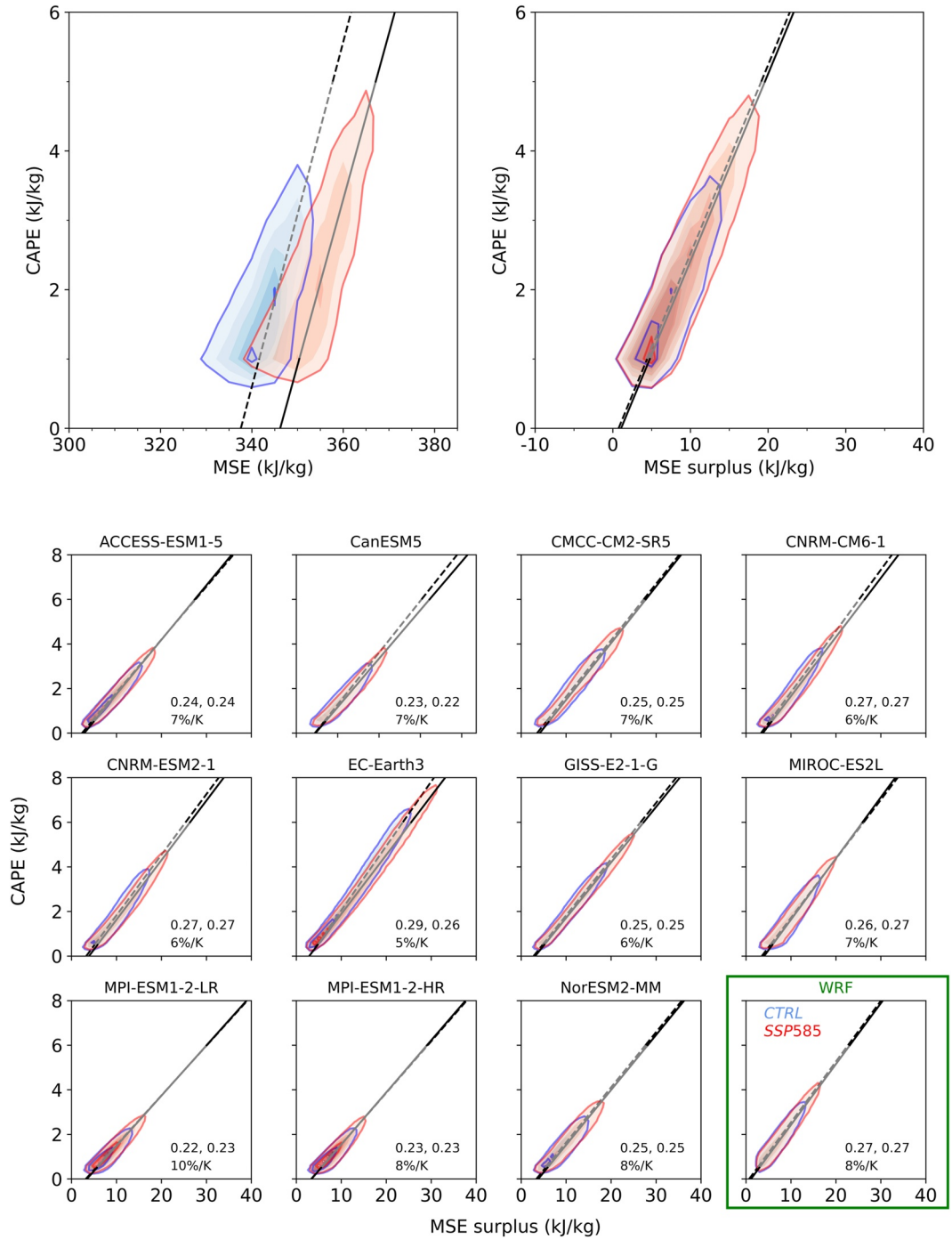

Figure 3. (Top) Relationships between CAPE and surface MSE (left) and MSE surplus (right), for WRF runs in N. America summertime (MJJA), showing all cases where CAPE >1,000 J/kg (CTRL = blue, dotted; PGW = red, solid). Lines are fitted orthogonal regressions. Color shading increments are 1.5% for the left panel and 0.75% for the right. The CAPE-MSE surplus relationship is robust across climate states. (Bottom) CAPE–MSE surplus relationships in 11 free-running CMIP6 models and WRF for N. American summertime (JJA), using all cases where CAPE >500 J/kg. Color shading increments are 0.5% for all models except EC-Earth3 (0.25%). The CAPE–MSE surplus relationship is robust in all models, even those with unrealistic CAPE.

exceeds some threshold, which changes between present and future simulations. This threshold, the x-intercept of the fitted regression, matches the mean minimum saturation MSE (h_m^*) in each climate state to within <0.3%. When CAPE is plotted against MSE surplus ($h_s - h_m^*$) instead, as in Equation 2, the relationship becomes robust across climate states and the residual variance becomes smaller, suggesting that this is a fundamental physical

relationship (Figure 3, top right). On both measures, variance and robustness, the CAPE-MSE surplus relationship of Equation 2 outperforms the expression based on dry static energy as in Agard and Emanuel (2017) and Li and Chavas (2021) (Figure S6 in Supporting Information S1, which shows both WRF runs and observations). Fitted slopes are nearly identical in WRF CTRL and PGW runs and in observations (0.27 in all), and intercepts are nearly zero (0.7, 1.1, and 1.6 kJ/kg for CTRL, PGW, and observations, respectively). In this perspective, the effects of climate change reduce to a greater sampling of conditions with high MSE surplus.

The relationship described by Equation 2 applies across all models tested and appears remarkably robust not only across climate states but across locations and times. It holds in 11 free-running climate models from the CMIP6 archive (Figure 3, bottom), though they differ strongly in their mean CAPE (Chavas & Li, 2022), CAPE distributions, and projected changes (from 5% to 10%/K). Their CAPE-MSE surplus relationships also differ slightly, with slopes of 0.22–0.29. Nevertheless, in each model that relationship remains constant across climate states. In the WRF model output, fitted slopes to CAPE versus MSE surplus remain similar when the data set is divided by latitude (northern vs. southern stations), by time of day (daytime vs. nighttime profiles), by interannual variations (anomalously warm vs. cold years), or even by season (winter vs. summer) (Figure S7 in Supporting Information S1).

3.4. A 3-Parameter Transformation

The robustness of Equation 2 across climate states suggests that model-projected CAPE changes result from relatively simple adjustments. The fitted slope for each model, A, is a function of the shape of the environmental profile; for A to remain constant, that shape must not alter much. Changes in CAPE in Equation 2 can then result only from changes in surface conditions (h_s, which depends on surface temperature and humidity), or in a single metric of temperature in the free troposphere (h_m^*). While the quantile ratio plot in Figure 1 shows that transformations based on one or two parameters are insufficient for describing CAPE distributional changes, it appears that three parameters may be sufficient.

To construct our scaling, we use the two effects that produce the shift in CAPE contours in T–H space seen in Section 3.2—an overall surface warming and a small decrease in mean lapse rates—and add the small but significant change in surface relative humidity in our WRF runs (−0.9%; see Figure S8 in Supporting Information S1 for its effect). As described in Methods, we calculate mean changes in these three parameters across our domain and apply them to the CTRL profiles. This simple adjustment correctly produces the shifting CAPE-MSE relationship, matching its slope and x-intercept (Figure 4, left). It also reproduces both the distributional narrowing and the magnitude of

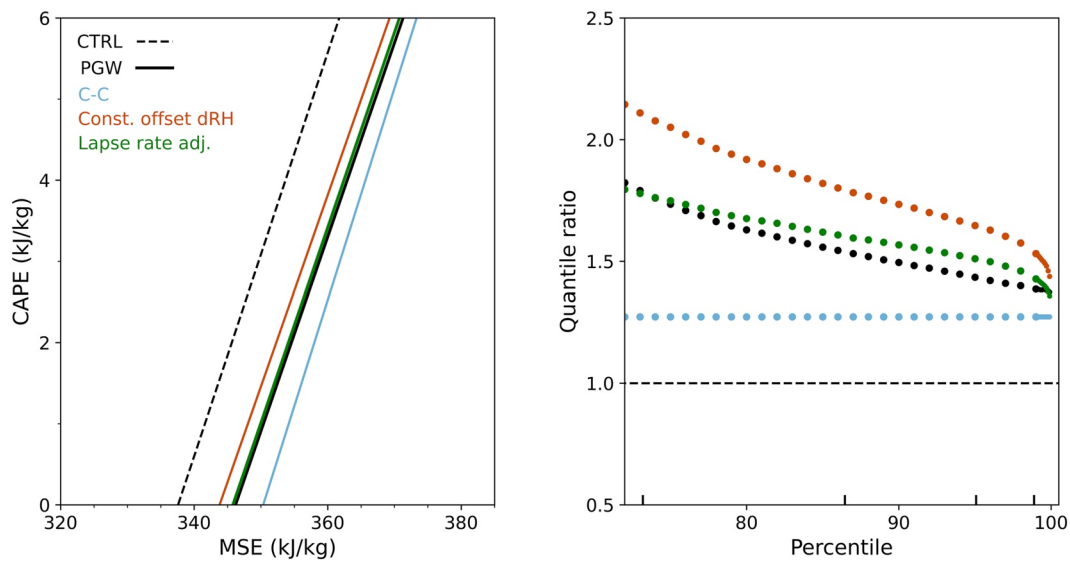

Figure 4. Comparison of present and future CAPE in model output (black) and synthetics: *C–C scaling* (light blue), *constant offset* including an RH adjustment (orange), and *lapse rate adjustment* (green). (Left) Fitted regression lines of the future CAPE-MSE relationship as in Figure 3. See Table S2 in Supporting Information S1 for slopes and x-intercepts. (Right) Future changes in CAPE as quantile ratio plots, as in Figure 1. The simple *lapse rate adjustment* effectively reproduces CAPE distributional changes.

CAPE change for the high-CAPE conditions of interest (Figure 4, right). While midlatitudes CAPE is highly heterogeneous, a relatively straightforward transformation can capture its full distributional change in a future warmer climate.

4. Discussion

Increases in severe weather events, which are associated with high CAPE, are a substantial societal concern under global warming. Their understanding has been hindered by lack of a widely accepted theory or framework to describe midlatitudes CAPE changes. Theories developed for the convective tropics (e.g., Singh & O'Gorman, 2013) are not appropriate for midlatitudes land, where advection and a strong diurnal cycle mean that the mid-troposphere is often decoupled from the surface (Figure S9 in Supporting Information S1). In this work, we show that Equation 2, a modified version of the heat-engine theory originally proposed in 1996 (EB96) and of its later extensions (AE17, LC21), provides a compact representation of midlatitudes CAPE that is robust across space, over diurnal and seasonal cycles, and across climate states.

We term the work developed here a framework rather than a theory because the transformation requires empirical values and we do not predict the slope A, which accounts for the shape of the environmental profile and is empirically fit. Similarly, AE17 would require an empirical correction to their slope for a realistic moist atmosphere. In EB96, by contrast, A is based on thermodynamics and is effectively the Carnot efficiency of the atmosphere. In our WRF runs, the empirical slope of the CAPE-MSE relationship is larger than Carnot (0.24, vs. 0.14 for Carnot as defined by EB96), but this is not a violation of the second Law given our focus on highly convective conditions.

Any transformation that describes changes in midlatitudes CAPE will necessarily require at least three parameters, one more than SO13, because the midlatitudes free troposphere cannot be predicted from surface T and RH even on average. In this work we find that *only* three parameters are required: three regional mean values across our domain are sufficient to capture the full distributional change in the CAPE >73rd quantile. This result may seem counterintuitive, since present-day North America encompasses a wide range of environmental conditions, future climate changes are spatially variable, and the response of CAPE is highly nonlinear. However, CAPE develops appreciably only in a relatively restricted subset of T–H space, where changes are more uniform.

The CAPE changes projected in our WRF runs and in most CMIP6 models are higher than Clausius-Clapeyron, the expectation under RCE. This difference matters for occurrence of extreme conditions. Incidences of summertime CAPE >2000 J/kg, a commonly-used threshold for severe weather, rise half again as much in our WRF projections as under C–C scaling (14% in CTRL; >24% in PGW, 20% in *C–C*). Of course, predicting how this rise in extreme CAPE will affect future severe weather requires also understanding how it will map to a change in convective updraft velocities—but understanding CAPE changes under CO_2-induced warming is a necessary first step. The dependence of CAPE on MSE surplus provides a simple but robust framework for predicting and understanding that response.

Acknowledgments
The authors thank Dan Chavas, Tiffany Shaw, Funing Li, Zhihong Tan, and Osamu Miyawaki for constructive comments, and the National Center for Atmospheric Research (NCAR) for providing the WRF data set. We acknowledge the World Climate Research Programme, which, through its Working Group on Coupled Modelling, coordinated and promoted CMIP6. We thank the climate modeling groups for producing and making available their model output, the Earth System Grid Federation (ESGF) for archiving the data and providing access, and the multiple funding agencies who support CMIP6 and ESGF. This work is supported by the Center for Robust Decision-making on Climate and Energy Policy (RDCEP), funded by the NSF Decision Making Under Uncertainty program, Award SES-1463644, and was completed in part with resources provided by the University of Chicago Research Computing Center.

Data Availability Statement

The 4-km WRF convection-permitting model output can be downloaded from NCAR RDA (https://rda.ucar.edu/datasets/ds612.0/). The IGRA radiosonde data can be downloaded from NOAA (https://www.ncei.noaa.gov/products/weather-balloon/integrated-global-radiosonde-archive). CMIP6 model output is available from the Earth System Grid Federation (ESGF, https://esgf-node.llnl.gov/projects/cmip6/).

References

Agard, V., & Emanuel, K. (2017). Clausius–Clapeyron scaling of peak CAPE in continental convective storm environments. *Journal of the Atmospheric Sciences*, *74*(9), 3043–3054. https://doi.org/10.1175/JAS-D-16-0352.1

Brooks, H. E., Anderson, A. R., Riemann, K., Ebbers, I., & Flachs, H. (2007). Climatological aspects of convective parameters from the NCAR/NCEP reanalysis. *Atmospheric Research*, *83*(2), 294–305. https://doi.org/10.1016/j.atmosres.2005.08.005

Brooks, H. E., Lee, J. W., & Craven, J. P. (2003). The spatial distribution of severe thunderstorm and tornado environments from global reanalysis data. *Atmospheric Research*, *67–68*, 73–94. https://doi.org/10.1016/S0169-8095(03)00045-0

Chavas, D. R., & Li, F. (2022). Biases in CMIP6 historical U.S. severe convective storm environments driven by biases in mean-state near-surface moist static energy. *Geophysical Research Letters*, *49*(23), e2022GL098527. https://doi.org/10.1029/2022GL098527

Chen, J., Dai, A., Zhang, Y., & Rasmussen, K. L. (2020). Changes in convective available potential energy and convective inhibition under global warming. *Journal of Climate*, *33*(6), 2025–2050. https://doi.org/10.1175/JCLI-D-19-0461.1

Diffenbaugh, N. S., Scherer, M., & Trapp, R. J. (2013). Robust increases in severe thunderstorm environments in response to greenhouse forcing. *Proceedings of the National Academy of Sciences of the United States of America*, *110*(41), 16361–16366. https://doi.org/10.1073/pnas.1307758110

Emanuel, K. (1994). *Atmospheric convection*, (Vol. Chap. 6, pp. 169–175). Oxford University Press.

Emanuel, K., & Bister, M. (1996). Moist convective velocity and buoyancy scales. *Journal of the Atmospheric Sciences*, *53*(22), 3276–3285. https://doi.org/10.1175/1520-0469(1996)053⟨3276:MCVABS⟩2.0.CO;2

Eyring, V., Bony, S., Meehl, G. A., Senior, C. A., Stevens, B., Stouffer, R. J., & Taylor, K. E. (2016). Overview of the coupled model intercomparison project phase 6 (CMIP6) experimental design and organization. *Geoscientific Model Development*, *9*(5), 1937–1958. https://doi.org/10.5194/gmd-9-1937-2016

Gettelman, A., Seidel, D. J., Wheeler, M. C., & Ross, R. J. (2002). Multidecadal trends in tropical convective available potential energy. *Journal of Geophysical Research*, *107*(D21), ACL17–1–ACL17–8. https://doi.org/10.1029/2001JD001082

Groenemeijer, P. H., & van Delden, A. (2007). Sounding-derived parameters associated with large hail and tornadoes in The Netherlands. *Atmospheric Research*, *83*(2), 473–487. https://doi.org/10.1016/j.atmosres.2005.08.006

Johns, R. H., Doswell, I., & Charles, A. (1992). Severe local storms forecasting. *Weather and Forecasting*, *7*(4), 588–612. https://doi.org/10.1175/1520-0434(1992)007⟨0588:SLSF⟩2.0.CO;2

Kaltenböck, R., Diendorfer, G., & Dotzek, N. (2009). Evaluation of thunderstorm indices from ECMWF analyses, lightning data and severe storm reports. *Atmospheric Research*, *93*(1), 381–396. https://doi.org/10.1016/j.atmosres.2008.11.005

Kunz, M. (2007). The skill of convective parameters and indices to predict isolated and severe thunderstorms. *Natural Hazards and Earth System Sciences*, *7*(2), 327–342. https://doi.org/10.5194/nhess-7-327-2007

Lepore, C., Abernathey, R., Henderson, N., Allen, J. T., & Tippett, M. K. (2021). Future global convective environments in CMIP6 models. *Earth's Future*, *9*(12), e2021EF002277. https://doi.org/10.1029/2021EF002277

Li, F., & Chavas, D. R. (2021). Midlatitude continental CAPE is predictable from large-scale environmental parameters. *Geophysical Research Letters*, *48*(8), e2020GL091799. https://doi.org/10.1029/2020GL091799

Liu, C., Ikeda, K., Rasmussen, R., Barlage, M., Newman, A. J., Prein, A. F., et al. (2017). Continental-scale convection-permitting modeling of the current and future climate of North America. *Climate Dynamics*, *49*(1), 71–95. https://doi.org/10.1007/s00382-016-3327-9

Miyawaki, O., Shaw, T. A., & Jansen, M. F. (2022). Quantifying energy balance regimes in the modern climate, their link to lapse rate regimes, and their response to warming. *Journal of Climate*, *35*(3), 1045–1061. https://doi.org/10.1175/JCLI-D-21-0440.1

Moncrieff, M. W., & Miller, M. J. (1976). The dynamics and simulation of tropical cumulonimbus and squall lines. *Quarterly Journal of the Royal Meteorological Society*, *102*(432), 373–394. https://doi.org/10.1002/qj.49710243208

Muller, C. J., O'Gorman, P. A., & Back, L. E. (2011). Intensification of precipitation extremes with warming in a cloud-resolving model. *Journal of Climate*, *24*(11), 2784–2800. https://doi.org/10.1175/2011JCLI3876.1

Rasmussen, K. L., Prein, A. F., Rasmussen, R. M., Ikeda, K., & Liu, C. (2017). Changes in the convective population and thermodynamic environments in convection-permitting regional climate simulations over the United States. *Climate Dynamics*, *55*(1–2), 383–408. https://doi.org/10.1007/s00382-017-4000-7

Rasmussen, & Liu, C. (2017). *High resolution WRF simulations of the current and future climate of North America*. Research Data Archive at the National Center for Atmospheric Research, Computational and Information Systems Laboratory. https://doi.org/10.5065/D6V40SXP

Romps, D. M. (2011). Response of tropical precipitation to global warming. *Journal of the Atmospheric Sciences*, *68*(1), 123–138. https://doi.org/10.1175/2010JAS3542.1

Romps, D. M. (2016). Clausius–Clapeyron scaling of CAPE from analytical solutions to RCE. *Journal of the Atmospheric Sciences*, *73*(9), 3719–3737. https://doi.org/10.1175/JAS-D-15-0327.1

Schwarzwald, K., Poppick, A., Rugenstein, M., Bloch-Johnson, J., Wang, J., McInerney, D., & Moyer, E. J. (2021). Changes in future precipitation mean and variability across scales. *Journal of Climate*, *34*(7), 2741–2758. https://doi.org/10.1175/JCLI-D-20-0001.1

Seeley, J. T., & Romps, D. M. (2015). Why does tropical convective available potential energy (CAPE) increase with warming? *Geophysical Research Letters*, *42*(23), 10429–10437. https://doi.org/10.1002/2015GL066199

Singh, M. S., & O'Gorman, P. A. (2013). Influence of entrainment on the thermal stratification in simulations of Radiative-Convective Equilibrium. *Geophysical Research Letters*, *40*(16), 4398–4403. https://doi.org/10.1002/grl.50796

Singh, M. S., & O'Gorman, P. A. (2015). Increases in moist-convective updraught velocities with warming in Radiative-Convective Equilibrium: Increases in updraught velocities with warming. *Quarterly Journal of the Royal Meteorological Society*, *141*(692), 2828–2838. https://doi.org/10.1002/qj.2567

Sun, X., Xue, M., Brotzge, J., McPherson, R. A., Hu, X.-M., & Yang, X.-Q. (2016). An evaluation of dynamical downscaling of central plains summer precipitation using a WRF-based regional climate model at a convection-permitting 4 km resolution. *Journal of Geophysical Research: Atmospheres*, *121*(23), 13801–13825. https://doi.org/10.1002/2016JD024796

Trapp, R. J., Diffenbaugh, N. S., & Gluhovsky, A. (2009). Transient response of severe thunderstorm forcing to elevated greenhouse gas concentrations. *Geophysical Research Letters*, *36*(1), L01703. https://doi.org/10.1029/2008GL036203

Wang, Z., Franke, J. A., Luo, Z., & Moyer, E. J. (2021). Reanalyses and a high-resolution model fail to capture the "high tail" of CAPE distributions. *Journal of Climate*, *34*(21), 8699–8715. https://doi.org/10.1175/JCLI-D-20-0278.1

Williams, E., & Renno, N. (1993). An analysis of the conditional instability of the tropical atmosphere. *Monthly Weather Review*, *121*(1), 21–36. https://doi.org/10.1175/1520-0493(1993)121⟨0021:AAOTCI⟩2.0.CO;2

Ye, B., Del Genio, A. D., & Lo, K. K.-W. (1998). CAPE variations in the current climate and in a climate change. *Journal of Climate*, *11*(8), 1997–2015. https://doi.org/10.1175/1520-0442-11.8.1997

Zhang, Y., & Boos, W. R. (2023). An upper bound for extreme temperatures over midlatitude land. *Proceedings of the National Academy of Sciences*, *120*(12), e2215278120. https://doi.org/10.1073/pnas.2215278120

Zhou, W., & Xie, S.-P. (2019). A conceptual spectral plume model for understanding tropical temperature profile and convective updraft velocities. *Journal of the Atmospheric Sciences*, *76*(9), 2801–2814. https://doi.org/10.1175/jas-d-18-0330.1